

◎ 論 文

Effect of Parametric Excitation on Lateral Vibrations of Long, Slender Marine Structures

Han Il Park*

(1992년 12월 20일 접수)

장주형 해양구조물의 횡방향 진동에 대한 파라메트릭 가진의 효과

박 한 일*

Key Words : 장주형 해양구조물(Long, slender marine structure), 횡방향 진동(Lateral vibration), 파라메트릭 가진(Parametric excitation), 결합 가진(Combined excitation), Mathieu 안정차트(Mathieu stability chart)

초 록

본 연구에서는 장주형 해양구조물의 횡방향 진동에 대한 파라메트릭 가진의 효과를 고찰하였다. 먼저, 장주형 해양구조물의 횡방향 운동에 대한 4계 편미방지배방정식을 비선형 Mathieu 방정식으로 유도하였다. 비선형 Mathieu 방정식의 해를 구하여 장주형 해양구조물의 동적 반응 특성을 해석하였다. 유체 비선형 감쇠력은 불안정 조건하에 있는 파라메트릭 진동의 반응크기를 제한 하는데 중요한 역할을 한다. 파라메트릭 진동의 경우 가장 큰 반응크기는 Mathieu 안정차트의 첫번째 불안정 구간에서 일어난다. 반면에, 파라메트릭 진동과 강제진동의 결합 진동인 경우, 가장 큰 반응 크기는 두번째 불안정 구간에서 발생된다. 파라메트릭 가진으로 인한 장주형 해양구조물의 횡방향 운동은 동적조건에 따라 subharmonic, superharmonic 또는 chaotic 운동이 되기도 한다.

INTRODUCTION

This research has been initially intended to analyse the interaction between ocean superstructures and mounted slender marine structures such as rigid risers, TLP tethers. Figure 1 shows

some typical examples of such systems ; a vertical marine riser deployed from a drilling vessel and tethers of a tension leg platform. As the first step to this research, the dynamic behaviours of the slender marine structures are analysed in this work.

These slender marine structures are subject-

* 한국해양대학교, 이공대학, 해양공학과

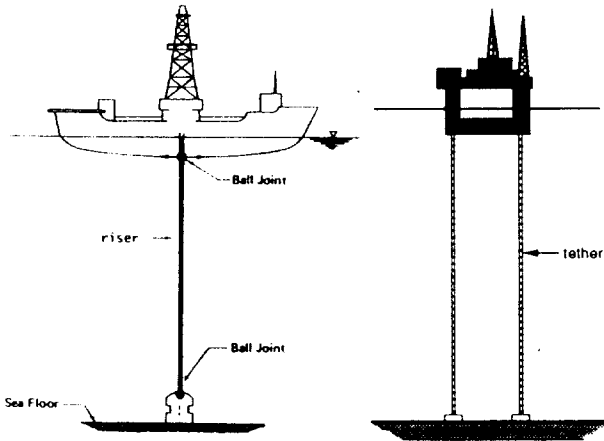


Fig. 1 Drilling Vessel and Tension Leg Platform Systems

ted to several kinds of excitation. The main sources of the excitation are the vertical (causing parametric excitation) and lateral (inducing forcing excitation) forces of their top mounting point imparted by heave and surge motions of the surface platform respectively. When lateral forces are considered only in the dynamic analysis of the structures, the lateral motion becomes forced vibrations or a forcing excitation problem. Much research work has been carried out on this problem—see references.^{1)–3)} Meanwhile, when the vertical forces, that is, time-varying axial forces are taken into account only, the resulting motion becomes parametrically excited vibrations (the Mathieu stability problem). There has been some research on the problem such as Hsu⁴⁾ and Patel and Park.⁵⁾

However, when the vertical and lateral forces are simultaneously considered, which is more realistic, the dynamic behaviour of the slender marine structures becomes a combined parametric and forcing excitation problem. Compared to forcing or parametric excitation, research on combined excitation has only recently been carried out over the last two decades—see references^{6)–7)}

and therein references. Other than those of marine structures, there are some examples of systems under combined excitation such as mechanisms on vibrating foundations, ship rolling motion by following or oblique seas, load motion of a crane vessel, yaw motion of tension leg platform by head seas, etc. In this paper, as the result of parametric excitation effect on the lateral vibrations of slender marine structures, the combined excitation problem will also be studied.

THEORETICAL APPROACH

The slender vertical marine structure considered in this work is idealised as a straight, simply supported column of uniform cross section. Figure 2 shows the idealised configuration under combined excitation and gives the notation to be used. For this kind of marine structure, a governing equation of lateral motion can be written as

$$M \frac{\partial^2 y}{\partial t^2} + EI \frac{\partial^4 y}{\partial x^4} - [T_0 + g(t)] \frac{\partial^2 y}{\partial x^2} + B_v \left| \frac{\partial y}{\partial t} \right| \frac{\partial y}{\partial t} = 0 \dots\dots\dots (1)$$

where M is the total mass per unit length of the structure segment, EI is the structure flexural rigidity, T_0 is constant axial tension, $g(t)$ is the function of time-varying axial forces and $B_v = 0.5 C_D \rho_w d_o$, where C_D is a drag coefficient, d_o is the outer diameter of the structure and ρ_w is sea water density. It is noted that since this research intended to analyse the complicated parametric excitation effect on vibrations of slender marine structures, other physical terms which can be included in the governing equation¹⁾ are simplified.

The partial differential equation¹⁾ is reduced to an ordinary non-linear differential equation by using the method of separation of variables. As can be seen in Figure 2, since both ends of the

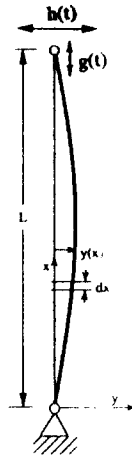


Fig. 2 Model structure configuration and notation.

structure are pin-jointed, its modes of motion can be readily reduced to a rigid body mode and sinusoidal elastic response modes. Then an approximate solution to equation¹⁾ is written in the form

$$y(t) = h(t) \frac{x}{L} + \sum_{n=1}^{\infty} f_n(t) \sin \frac{n\pi x}{L} \dots\dots\dots (2)$$

where L is the length of the structure, $f_n(t)$ is an unknown function of the elastic response modes (a generalised coordinate) and $h(t)$ is a prescribed lateral motion of the top end of the structure imparted by surface platform surge motion.

Substituting equations²⁾ into equation¹⁾ multiplying the resulting equation throughout by $\sin(n\pi x/L)$ and integrating over the length of the structure gives

$$\begin{aligned} & \frac{ML}{2} \frac{d^2 f_m}{dt^2} + \left[EI \left(\frac{m\pi}{L} \right)^4 \frac{L}{2} + \{T_o + g(t)\} \left(\frac{m\pi}{L} \right)^2 \frac{L}{2} \right] f_m \\ & + B_v \int_0^L \left| \frac{x}{L} \frac{dh}{dt} + \sum_{n=1}^{\infty} \left(\sin \frac{n\pi x}{L} \frac{df_n}{dt} \right) \right| \\ & \left\{ \frac{x}{L} \frac{dh}{dt} + \sum_{n=1}^{\infty} \left(\sin \frac{n\pi x}{L} \frac{df_n}{dt} \right) \right\} \sin \frac{n\pi x}{L} dx \end{aligned}$$

$$= - \frac{LM}{m\pi} (-1)^m \frac{d^2 h}{dt^2} \dots\dots\dots (3)$$

In deriving equation³⁾ the following integrations are used.

$$\begin{aligned} \int_0^L \sin \frac{m\pi x}{L} dx &= - \frac{L^2}{m\pi} (-1)^m \\ \int_0^L \sin \frac{m\pi x}{L} \sin \frac{n\pi x}{L} dx &= \frac{L}{2} \text{ for } n=m \\ &= 0 \text{ for } n \neq m \end{aligned}$$

Rearranging equation³⁾ gives

$$\begin{aligned} & \frac{d^2 f_m}{dt^2} + \left[\bar{\omega}_m^2 + \frac{1}{M} \left(\frac{m\pi}{L} \right)^2 g(t) \right] f_m \\ & + \frac{2B_v}{ML} \int_0^L \left| \frac{x}{L} \frac{dh}{dt} + \sum_{n=1}^{\infty} \left(\sin \frac{n\pi x}{L} \frac{df_n}{dt} \right) \right| \\ & \left\{ \frac{x}{L} \frac{dh}{dt} + \sum_{n=1}^{\infty} \left(\sin \frac{n\pi x}{L} \frac{df_n}{dt} \right) \right\} \sin \frac{n\pi x}{L} dx \\ & = \frac{-2(-1)^m}{m\pi} \frac{d^2 h}{dt^2} \dots\dots\dots (4) \end{aligned}$$

where

$$\bar{\omega}_m^2 = \frac{EI}{M} \left[\frac{n\pi x}{L} \right]^4 + \frac{T_o}{M} \left[\frac{n\pi x}{L} \right]^2 \dots\dots\dots (5)$$

Equation⁴⁾ seems to be very complicated to analyse, especially due to the existence of the parametric excitation term. In order to analyse the complicated excitation problems, further assumptions are made. First, of the elastic response modes, only the predominant fundamental (first) mode is considered. The assumption of employing only the fundamental mode shape has been justified experimentally by Somerset and Evan-Iwanowski.⁸⁾ Secondly, the functions of surge induced top end lateral motion, $h(t)$ and heave induced time-varying axial forces becomes more regular due to the transfer function from wave action to structural forces. $g(t)$ are assumed to be sinusoidal. The assumption is based on the fact that

even if ocean waves are irregular, the time-varying axial forces. In addition, this research is concerned with large long period waves which tend to be more narrow banded in spectral content.

The initial boundary condition of the top end is set to be in the middle point of surge motion and in the lowest position of heave motion. In addition, the top end is taken to rotate in the clockwise direction by the wave-induced surface platform motion. Therefore, $h(t)$ and $g(t)$ can be put to be

$$h(t) = -y_0 \sin \omega t \text{ and } g(t) = -S \cos \omega t \dots\dots\dots (6)$$

where y_0 and S are respectively the amplitudes of top end lateral displacements and timevarying axial forces, and ω is the angular frequency of the top end motion. Note that since they both stem from a single source, the angular frequencies of the two excitations are the same.

It is useful to introduce a nondimensional time such as $\tau = \omega t$. Then, equation⁴⁾ finally takes the form

$$\begin{aligned} & \frac{d^2 f}{d\tau^2} + (\alpha - \beta \cos \tau) f \\ & + C_1 \int_0^L \left\{ C_2 X \cos \tau + C_3 \sin \frac{\pi x}{L} \frac{df}{d\tau} \right\} \\ & \left\{ C_2 X \cos \tau + C_3 \sin \frac{\pi x}{L} \frac{df}{d\tau} \right\} \sin \frac{\pi x}{L} dx \\ & = - \frac{2y_0}{\pi} \sin \tau \dots\dots\dots (7) \end{aligned}$$

where

$$\begin{aligned} \alpha &= \left(\frac{\bar{\omega}}{\omega}\right)^2, \quad \beta = \frac{S}{EI(\pi/L)^2 + T_0} \left(\frac{\bar{\omega}}{\omega}\right)^2, \quad C = \frac{8B_v}{3\pi M} \\ C_2 &= - \frac{\sqrt{3x} y_0}{2L \sqrt{L}}, \quad C_3 = \frac{\sqrt{3x}}{2\sqrt{L}} \dots\dots\dots (8) \end{aligned}$$

Equation⁷⁾ represents vibrations of the structure subjected to combined parametric and forcing

excitation. The lateral response of the structure is strongly depends upon the β/α and y_0 which are referred here as the strengths of parametric excitation and forcing excitation respectively. The hydrodynamic damping related coefficient, c plays a role in limiting the response of combined excitation. If f is obtained by solving equation,⁷⁾ the lateral responses of the structure under combined excitation can be obtained by substituting f into equation.²⁾ At the present time, adequate techniques are not available to give an analytical solution of equation,⁷⁾ especially for large values of α and β . Therefore, it is necessary to employ a numerical method.

Before carrying out a numerical analysis, it is worthwhile examining equation⁷⁾ further. First, if the time-varying axial force, $S \cos \omega t$, is not considered, that is, $\beta = 0$ from equation,⁸⁾ the resulting motion of the structure becomes forced vibrations. An analytical solution of the forced vibration problem can be obtained by iteration procedures.²⁾

A resonance occurs when the forcing angular frequency, ω , is equal to the natural frequencies, $\bar{\omega}$. However, when the hydrodynamic damping force is considered, the amplitude of a resonance response is limited.

Second, if the lateral motion of the top end is not considered, that is, if y_0 is zero, equation⁷⁾ becomes

$$\frac{d^2 f}{d\tau^2} + (\alpha - \beta \cos \tau) f + C \left| \frac{df}{d\tau} \right| \frac{df}{d\tau} = 0 \dots\dots\dots (9)$$

by using the following integral

$$\int_0^L \left| \sin \frac{\pi x}{L} \right| \sin \frac{\pi x}{L} \sin \frac{\pi x}{L} dx = \frac{4L}{3\pi}$$

Equation⁹⁾ is the non-linear Mathieu equation and describes parametrically excited vibrations of the structure.

When the hydrodynamic damping force is excluded, the response of parametric excitation become stable or unstable according to the combination of parameters, α and β . This fact results in creating the Mathieu stability chart(Figure 3).

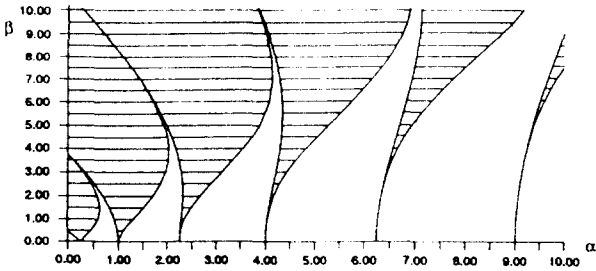


Fig. 3 Mathieu stability chart(shaded areas are unstable).

Patel and Park⁵⁾ created for the first time the Mathieu chart for large values of α and β which is necessary for the dynamic analysis of highly tensioned slender structures and structural pulse buckling.

However, when the non-linear hydrodynamic damping force is included, even unstable solutions are limited. An approximate analytical solution can be obtained for small values of the parameters, α and β , by using perturbation techniques and can be expressed in the form—see references 9 and 5 for further details.

$$f(\tau) = a_N \cos\left(\frac{Nt}{2} + \theta_N\right) + (\text{Higher order terms}) \dots\dots\dots (10)$$

where N is a positive integer and indicates the number of the instability region along the α axis of the Mathieu stability chart.

For example, in the first instability region, the steady state amplitude, a_1 , and the phase angle, θ_1 , become

$$a_1 = \frac{3\pi}{4C} \sqrt{\beta^2 - 4(\alpha - 0.25)^2}$$

$$\theta_1 = 0.5 \cos^{-1}\left(\frac{2}{\beta}(\alpha - 0.25)\right)$$

As can be seen from equation¹⁰⁾ the response of parametric excitation becomes subharmonic (in the first instability region, that is, $N=1$), harmonic ($N=2$) or superharmonic ($N>2$). This result will be shown later. It is, however, noted that there exist some special cases where the response motion of parametric excitation becomes chaotic which was shown in the reference.¹⁰⁾ Figure 4 illustrates one example of such chaotic motion. Therefore there remains further research into identifying the detailed response characteristic of parametric excitation.

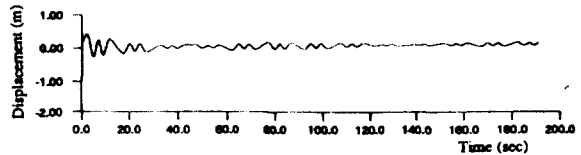


Fig. 4 One Example of Chaotic Motion for Parametric Excitation

RESULTS AND DISCUSSION

Equation⁹⁾ which describes a combined excitation problem, is solved using the fourth-order Runge-Kutta method with an extension to Romberg's integration method. The results of this research are illustrated for three typical values of α and ω given in Table 1. Here drag coefficient C_d is assigned to be 0.8. The worst sea state is an important environmental condition for the design of marine structures and is thus considered here. In such a condition, 15 seconds is a typical ocean wave period and is used here as an excita-

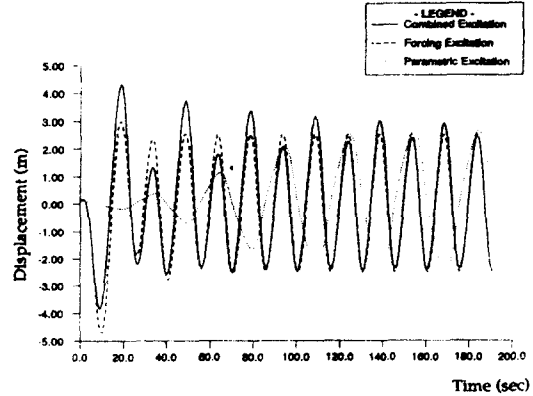
Table 1. Values of Each Excitation Parameter for Three Cases

Excitation	Case I	Case II	Case III
Forcing	$\alpha = 0.25$ $y_0 = 3.0\text{m}$	$\alpha = 1.0$ $y_0 = 3.0\text{m}$	$\alpha = 6.53$ $y_0 = 3.0\text{m}$
Parametric	$\alpha = 0.25$ $\beta = 0.25$	$\alpha = 1.0$ $\beta = 1.0$	$\alpha = 6.53$ $\beta = 6.53$
Combined	$\alpha = 0.25$ $\beta = 0.25$ $y_0 = 3.0\text{m}$	$\alpha = 1.0$ $\beta = 1.0$ $y_0 = 3.0\text{m}$	$\alpha = 6.53$ $\beta = 6.53$ $y_0 = 3.0\text{m}$

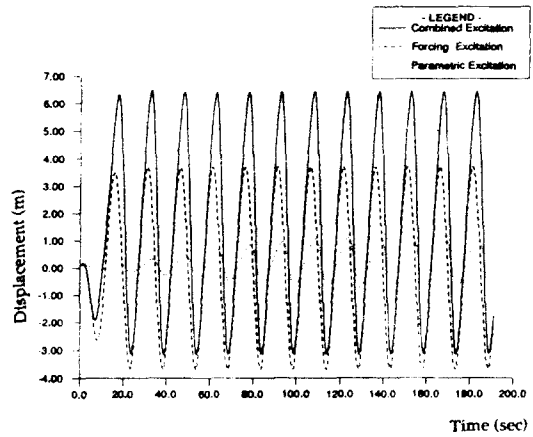
tion period. The amplitude of top end lateral displacement, y_0 , is assumed to be 3.0m which corresponds to RAO(the ratio amplitude operator) being 0.2 for 15.0m of ocean wave amplitude. The initial conditions employed in this study for the steady-state solutions are $f(0)=0.1$ and $df(0)/d\tau=0.0$.

As can be seen from Figure 3(Mathieu stability chart), the dynamic conditions for CASE I, II and III in Table 1 correspond to the first, second and fifth instability regions respectively. In order to investigate the effect of parametric excitation, comparisons between forcing, parametric and combined excitations are first made. For the validity of the comparison, the strengths of parametric excitation and forcing excitation, β/α and y_0 , are taken to be equal to 1.0 and 3.0m respectively for the three structures.

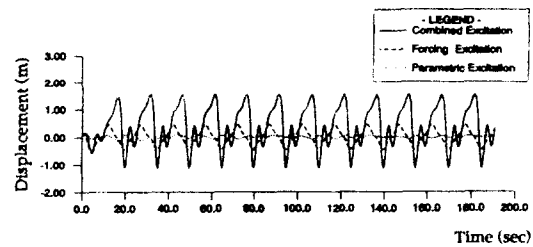
Figure 5(a) shows a comparison between forcing, parametric and combined excitations for the ASE I. The response amplitudes of three excitations are nearly identical at a steady state. It can be stated that in the first instability region there is no recognisable effect of the parametric excitation to increase the response amplitude of the dynamic system. Meanwhile, the response period of parametric excitation is double the excitation period. As was stated in the previous section, this means that the response motion of parametric excitation becomes subharmonic in the first instability



(a) Case I (First instability region)



(b) Case II (Second instability region)



(c) Case III (Fifth instability region)

Fig. 5 Comparison of Displacement Time Histories for Three Excitations

ity region. In the case of combined excitation, its response period is identical to the excitation period. However, if the strengths of excitations, β/α and y_0 , change, the response period of combined

excitation can also change.

Figure 5(b) presents results for the CASE II with a dominant dynamic condition falling under the second instability region. It can be seen from Figure 5(b) that the relative response amplitudes of three excitations in the second instability region are quite different from those in the first instability region (Figure 5(a)). In other words, in the second instability region, the response amplitudes of combined excitation are much larger than those of forcing or parametric excitation. This fact means that the effect of parametric excitations is significant in the second instability region. The response periods of the three excitations are all the same as the 15 second excitation period.

Figure 5(c) illustrates the result for the CASE III with a dominant dynamic condition which corresponds to being near the fifth instability region. The response amplitude of combined excitation is also much larger than that from forcing or parametric excitation as was for the CASE II. Figure 5(c) indicates that even though the responses of forcing or parametric excitation are small, those of combined excitation are relatively large. The response period of forcing excitation is still the same as the excitation period, 15 seconds. On the other hand, the response periods of parametric and combined excitations are small compared to the excitation period, that is, the parametric excitation causes the response of the dynamic system to be superharmonic in the higher instability regions.

In order to compare more clearly the response amplitudes of three excitations for different instability regions, many numerical calculations have been carried out. The absolute maximum response amplitude at steady state, $|f|_{\max}$ was obtained for several different set values of α and β instead of taking only three set values as in Figure 5. However, the strengths of excitations, $\beta/\alpha=1.0$

and $y_0=3.0\text{m}$ are kept as in Figure 5. Figure 6 shows the frequency response curves of forcing, parametric and combined excitations as functions of α values. A hydrodynamic damping force is considered in this research, so the responses are all limited.

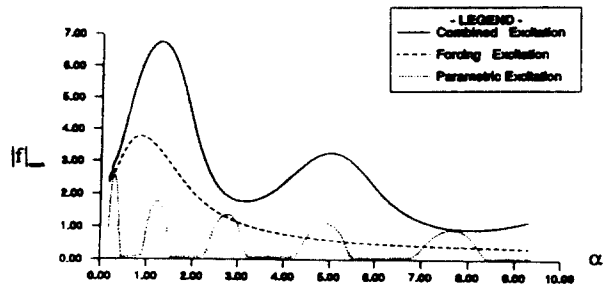


Fig. 6 Comparison of Frequency Response Curves for Three Excitations

In the case of parametric excitation, large response amplitudes occur in each instability region and their maximum value exists in the centre of each instability region with the magnitude of response amplitude decreasing for higher instability regions. The response diagram for combined excitation shows a quite different pattern from those for forcing and parametric excitations with this response being large in the even numbers of instability regions but relatively small in the odd numbers of instability regions.

The above comparison for three excitations shows that the effect of parametric excitation is significant to increase the lateral response of slender marine structures, especially in the even numbers of instability regions. This aspect means that parametric excitation needs to be considered in the dynamic analysis of slender marine structures.

CONCLUSION

This paper addresses one of preliminary results

of investigating the interaction between ocean superstructures and mounted long slender marine structures; the effect of parametric excitation on the lateral response of the slender structures. The parametric excitation induces the lateral motion of slender marine structures to be subharmonic, superharmonic or chaotic according to their dynamic conditions. By comparing response amplitudes of forcing excitation and combined excitation, it is known that the effect of parametric excitation is significant, especially in the even numbers of instability regions of the Mathieu stability chart. Therefore, in the dynamic analysis of tensioned slender marine structures, parametric excitation effect (time-varying axial forces or displacements) needs to be considered for more accurate results.

REFERENCES

- 1) Huang, T. and Dareing, D.T., "Buckling and lateral vibration of drill pipe", *Journal of Engineering for Industry*, 90, pp. 613-619, 1968.
- 2) Kirk, C.L., Etok, E.U. and Cooper, M.T., "Dynamic and static analysis of a marine riser", *Applied Ocean Research*, 1, pp. 125-135, 1979.
- 3) Kim, Y.C. and Triantafyllou, M.S., "The non-linear dynamics of long, slender cylinders", *Journal of Energy Resources Technology*, 106, pp. 250-256, 1984.
- 4) Hsu, C. S., "The response of a parametrically excited hanging string in fluid", *Journal of Sound and Vibration*, 39, pp. 305-316, 1975.
- 5) Patel, M.H. and Park, H.I., "Dynamics of tension leg platform tethers at low tension. Part I - Mathieu stability at Large parameters", *Marine Structures*, 4, pp. 257-273, 1991.
- 6) HaQuang, N. and Mook, D.T., "Non-linear structural vibrations under combined parametric and external excitations", *Journal of Sound and Vibration*, 118, pp. 291-306, 1987.
- 7) Plaut, R.H., Gentry, J.J. and Mook, D.T., "Non-linear structural vibrations under combined multi-frequency parametric and external excitations", *Journal of Sound and Vibration*, 140, pp. 381-390, 1990.
- 8) Somerset, J.H. and Evan-Iwanowski, R.M., "Experiments on parametric instability of columns", *Proceedings of the Second Southeastern Conference of Theoretical and Applied Mechanics*, Atlanta, Georgia, USA, pp. 503-525, 1964.
- 9) Minorsky, N., *Nonlinear oscillations*, Van Nostrand Company, Princeton, 1962.
- 10) Park, H.I., "Dynamic stability and vibrations of slender marine structures at low tension", Ph.D. thesis, University of London, 1992.